http://dx.doi.org/10.5012/bkcs.2013.34.10.3137

# Hydrogen Exchange Study of Winter Flounder Type I Antifreeze Protein

**Hee-Eun Kim, Ae-Ree Lee, Yeon-Mi Lee, Minjee Jeong, Chin-Ju Park,† and Joon-Hwa Lee***

*Department of Chemistry and RINS, Gyeongsang National University, Jinju, Gyeongnam 660-701, Korea*
**E-mail: joonhwa@gnu.ac.kr*
*†School of General Studies, Gwangju Institute of Science of Technology, Gwangju 500-712, Korea*
*Received June 19, 2013, Accepted July 25, 2013*

**Key Words :** NMR, Antifreeze protein, Hydrogen exchange, Ice-binding, Protein dynamics

Antifreeze proteins (AFPs) are found in various organisms, such as fish, insects, plants, bacteria, and fungi, to promote survival at subzero temperatures by decreasing the freezing point of bodily fluids.[1] AFPs, which are isolated from Arctic and Antarctic fish, comprise several structurally diverse classes of proteins and four classes of structurally independent proteins are identified: type I AFPs, alanine-rich α-helical proteins of 3.3 to 4.5 kDa;[2] type II AFPs, cysteine-rich globular proteins containing five disulfide bonds;[3] type III AFPs, 6-kDa globular proteins;[4] and Type IV AFPs, glutamate- and glutamine-rich α-helical proteins.[5]

The type I AFPs are alanine-rich amphiphilic α-helical proteins found in winter flounder, yellowtail flounder, Alaskan plaice, shorthorn sculpin, and Arctic sculpin.[1,2,6,7] The winter flounder AFP isoform, HPLC6, which is the most extensively studied AFP, contains three 11-amino acid repeats of the sequence Thr-$X_2$-Asx-$X_7$, where X is generally alanine.[2] X-ray crystallographic studies revealed that the type I AFP is completely α-helical in conformation, with the exception of the last residue (R37), which adopts a $3_{10}$-helix.[8] The hydroxyl and methyl groups of four threonine residues, particularly of the central two residues, T13 and T24, play key roles in the ice-binding properties of the type I AFP.[9] For example, T13S/T24S mutations of the type I AFP caused a 90-100% loss in activity relative to wild-type AFP.[9] The mutants, A17L and A21L, where the substitution lies adjacent to the Thr-rich face, caused a significant decrement of the thermal hysteresis activity, whereas the mutants A19L and A20L exhibited wild-type activity.[10] It was reported that termini of the HPLC6 isoform possess greater helix-stabilizing ability compared to the HPLC2 isoform, leading to a 50% difference in the thermal hysteresis activity between these two AFPs.[11] These results suggested that helical stabilization of the N and C termini is the critical component for antifreeze activity of the type I AFP.[11] It was recently reported that flexibility of the C-terminal region causes a loss of thermal hysteresis activity because its dynamic nature strongly prevents binding to the ice surface.[12]

Here, to further understand the correlation between the dynamic properties and function of type I AFPs, we performed NMR hydrogen exchange experiments on the winter flounder type I AFP (HPLC6 isoform) (Fig. 1, referred to as wt-AFP). The hydrogen exchange rate constants for the two mutants, A17L- and A20L-AFP (Fig. 1), which exhibit no and wild-type activities in thermal hysteresis respectively, are also determined. Comparison of the wt-AFP and mutant AFPs can provide valuable insights into the thermal hysteresis mechanism of type I AFPs.

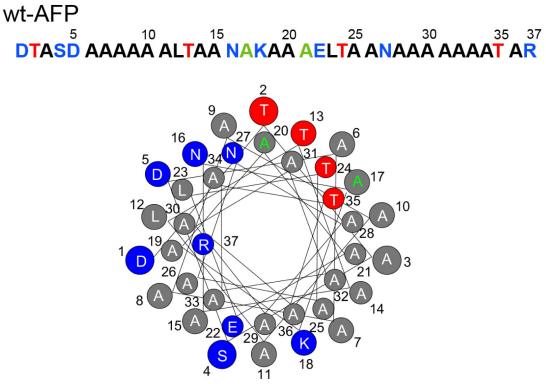


**Figure 1.** Amino acid sequence of winter flounder type I AFP (HPLC6 form) and its α-helical wheel representation.

## Experimental Section

The winter flounder type I AFP and its mutants, A17L- and A20L-AFPs, were purchased from Cosmo Genetech Inc. (Seoul, Korea) and desalted using a Sephadex G-25 gel filtration column. Each protein sample (5 mg) was dissolved in 500 μL of 90% $H_2O$/10% $D_2O$ NMR buffer containing 10 mM sodium phosphate (pH 8.0) and 100 mM NaCl.

The apparent longitudinal relaxation rate constants ($R_{1a} = 1/T_{1a}$) of the type I AFP and its mutants at various temperatures were determined using semi-selective inversion recovery 1D NMR experiments. The apparent relaxation rate constant of water ($R_{1w}$) was determined using a selective inversion recovery experiment, using a DANTE sequence for selective water inversion. $R_{1a}$ and $R_{1w}$ were determined using curve fitting of the inversion recovery data to the appropriate single-exponential function. The hydrogen exchange rate constants ($k_{ex}$) of the type I AFP and its mutants were determined using a water magnetization transfer experiment. The intensities of each exchangeable proton were measured with various delay times between the selective water inversion and detection pulses at 15 °C. The $k_{ex}$ for the amide and side-chain protons were determined by

fitting the data to Eq. (1):

$$\frac{I_0 - I(t)}{I_0} = 2\frac{k_{ex}}{(R_{1w} - R_{1a})}(e^{-R_{1a}t} - e^{-R_{1w}t}) \quad (1)$$

where $I_0$ and $I(t)$ are the intensities of the proton signal in the water magnetization transfer experiments at times zero and $t$, and $R_{1a}$ and $R_{1w}$ are the apparent longitudinal relaxation rate constants for the protein proton and water, respectively.

The hydrogen exchange rates were analyzed assuming an EX2 condition ($k_{cl} << k_{int}$) to understand relative proton accessibility or protection factor.[13] The hydrogen exchange reaction can be described by Eqn. 2:

$$N\text{-}H_{Closed} \underset{k_{cl}}{\overset{k_{op}}{\rightleftharpoons}} N\text{-}N_{Open} \xrightarrow{k_{int}} N\text{-}H^{*}_{Exchanged} \quad (2)$$

where $k_{op}$, $k_{cl}$, and $k_{int}$ are rate constants for opening, closing, and intrinsic exchange. For a stable protein structure under mild condition, such as no denaturant and not high temperature, the exchange rate can be expressed as $k_{ex} = K_{op} \cdot k_{int}$ ($K_{op} = k_{op}/k_{cl}$) at EX2 limit.[14] Under this condition, the fast equilibrium between open and closed states describes the extent of proton accessibility by the solvent and thus the protection factor (inverse of equilibrium constant, $P = 1/K_{op}$) reveals how well the proton is protected from solvent water.[13] The relative protection factor, $P_{relative}$ ($= P^{mut}/P^{wt}$), is determined from the exchange rate constants of the wt-AFP ($k_{ex}^{wt}$) and mutant AFPs ($k_{ex}^{mut}$) using the following equation: $P_{relative} = P^{mut}/P^{wt} = K_{op}^{wt}/K_{op}^{mut} = k_{ex}^{wt}/k_{ex}^{mut}$.

## Results and Discussion

Hydrogen exchange properties of the amide and side-chain protons were measured to probe differences in hydrogen bond strength between the winter flounder type I AFP (HPLC6 isoform) and its two mutants, A17L- and A20L-AFP. The partial assignment of the amide and side-chain resonances of wt-AFP was previously reported.[12,15] The two mutant AFPs were assigned by comparison of their NOESY and TOCSY spectra with the spectra for wt-AFP. The HPLC6 isoform of the winter flounder type I AFP is an Ala-rich protein (23 alanines in 37 amino acids, *see* Fig. 1(a)); most amide signals display a cluster in the range of 7.5 to 8.5 ppm (Fig. 2). Thus, only amide signals for S4 and N16/N27 are resolved in the amide proton spectra (Fig. 2). In addition, the signal for R37-Hη and two Hδ2 amide signals for the N16/N27 side-chains are also resolved in the amide proton spectra (Fig. 2).

The hydrogen exchange rate constants ($k_{ex}$) of the amide and side-chain protons were determined by using water magnetization transfer method at 15 °C. The $R_{1a}$ values were determined for the exchangeable protons of three AFPs by inversion recovery experiments with various delay times between selective inversion and detection pulses. The inversion recovery relaxation data for all protons of these three AFPs fit well to single exponentials. Figure 3 shows relative peak intensities for various protons in the water magnetization transfer spectra as a function of delay time between the selective water inversion and detection pulses for wt-AFP at 15 °C. Certain proton signals of the type I AFPs show large differences in peak intensities as a function of delay time after water inversion (Fig. 3). For example, the R37-Hη proton of the wt-AFP is rapidly exchanged and shows negative peak intensities at delay time ≥ 50 ms (Fig. 3D), whereas the side-chain resonances (Hδ21 and Hδ22) of the N16/N27 residues, which are the most slowly exchanging protons, exhibit positive peak intensities up to 100 ms (Fig. 3(c)). To avoid interference arising from NOEs with water, the intensity data with delay times less than 100 ms

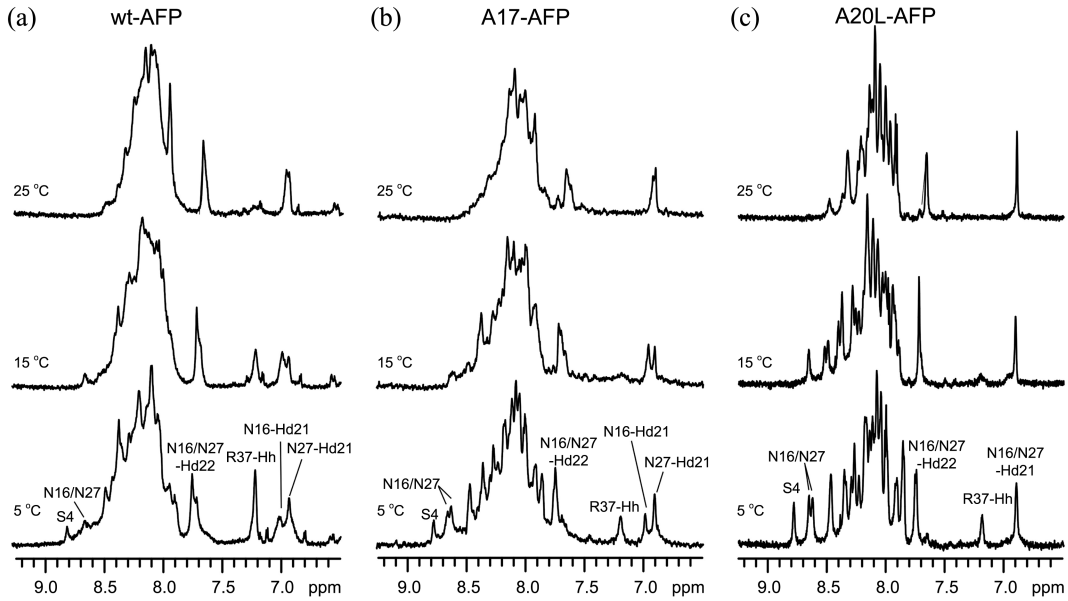


**Figure 2.** Temperature-dependent amide proton spectra of (a) wt-, (b) A17L-, and (c) A20L-AFPs. The experimental temperatures are shown on the left of spectra.

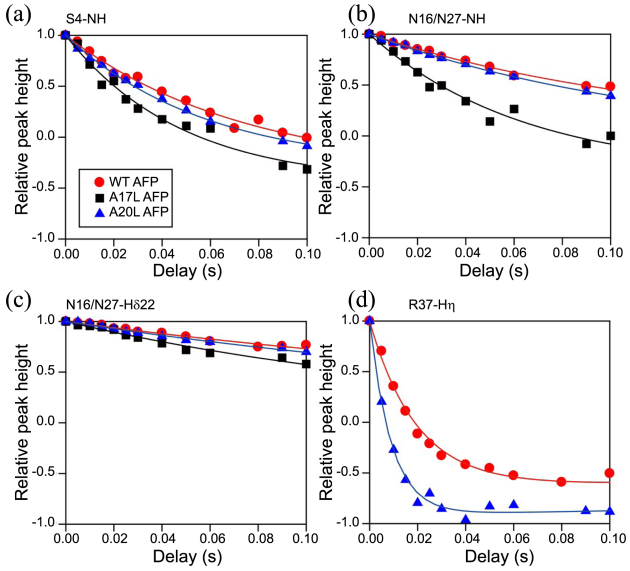


**Figure 3.** Relative peak height [$I(t)/I_0$] in the water magnetization transfer spectra for the (a) S4 and (b) N16/N27 amide protons and the (c) N16/N27-Hδ22 and (d) R37-Hη side-chains of the wt- (red circle), A17L- (black square), and A20L-AFPs (blue triangle) as a function of delay time at 15 °C. The solid lines indicate the best fitting data using Eq. (1).

were used to determine $k_{ex}$ by fitting to Eq. (1). The $k_{ex}$ values for certain protons studied here in the wt-AFP at 15 °C are given in Table 1. In wt-AFP, the amide protons of the S4 and N16/N27 residues have $k_{ex}$ of 9.2 ± 1.7 $s^{-1}$ and 3.9 ± 0.8 $s^{-1}$, respectively, at 15 °C. As expected, relatively rapid exchange is observed for the Hη side-chain proton on the C-terminal R37 residue at 15 °C ($k_{ex}$ = 51.4 ± 3.3 $s^{-1}$). Interestingly, the Hδ21 and Hδ22 side-chain protons of the N16 and N27 residues all exhibit exchange with solvent water ($k_{ex}$ < 2 $s^{-1}$) (Table 1).

The $k_{ex}$ values for certain protons were used to compare the effects of the A-to-L mutation at a specific site on hydrogen bond stabilities. In A17L-AFP, in which the Ala residue at postion 17 is changed to Leu, peak intensities of the N16/N27 amide protons exhibit larger dependence on the delay time after selective water inversion compared to the wt-AFP (Fig. 3(b)). This leads to a 1.5 - 2-fold larger $k_{ex}$ values of the N16/N27 amide signals than the corresponding protons in the wt-AFP protein (Table 1). The hydrogen exchange data demonstrate that the Leu side-chain at position 17 of A17L-AFP may interfere with hydrogen-bonding interaction of the amide proton of the neighboring N16 residue with the A20 carbonyl group when compared to the corresponding position 17 methyl group of wt-AFP. In addition, the relative protection factors ($P_{relative}$ = 0.8 and 0.5) for the N16/N27 amide protons indicate that these amide protons are well protected from solvent water in the wt-AFP. However, this solvent protection is affected by the A-to-L substitution at position 17 of the A17L-AFP. Similarly, the Hδ22 side-chain signals of the N16/N27 residues showed larger dependence on delay time after water inversion compared to wt-AFP (Fig. 3(c)), leading to approximately 2-fold greater $k_{ex}$ values for the N16/N27 Hδ22 side-chain protons in the A17L-AFP (Table 1).

The most striking result is that the $k_{ex}$ value (15.1 ± 3.3 $s^{-1}$) of the S4 amide proton is 2-fold larger than that of wt-AFP (Fig. 3(a) and Table 1), even though the S4 amide proton is located much farther from the L17 position in the α-helical structure (Fig. 1). In the A17L-AFP, the Hη side-chain proton on the C-terminal R37 residue exchanged too rapidly with solvent to be observed in the NMR spectra at ≥ 15 °C (Fig. 2(b)), indicating that this A-to-L substitution at position 17 also severely affects hydrogen exchange of the R37-Hη proton.

Hydrogen exchange experiments were also performed for A20L-AFP, where Ala residue at postion 20 is changed to Leu. In contrast to A17L-AFP, the A-to-L substitution at position 20 does not affect the $k_{ex}$ values of the N16/N27 amide protons (Fig. 3(b) and Table 1). This result indicates that the Leu side-chain at position 20 of A20L-AFP did not affect hydrogen-bonding interaction between the N16 amide proton and the L20 carbonyl group in contrast to A17L-AFP. In addition, there is no signficant effect of this substitution on hydrogen exchange for the S4 amide proton or N16/N27 side-chain protons (Fig. 3(a) and 3(c) and Table 1). The A-to-L substitution at position 20 caused only a little effect on exchange of the C-terminal R37 side-chain proton with solvent water (Fig. 3(d)), where the $k_{ex}$ value of the R37-Hη proton is approximately 2-fold larger for the A20L-AFP than the wt-AFP (Table 1).

The winter flounder type I AFP, 37-residue protein, contains three 11-amino acid repeats of the sequence Thr-$X_2$-Asx-$X_7$.[2,7] Four Thr residues, which are spaced at 11-residue intervals, play key roles in the ice-binding properties of the type I AFP, in which their linearly aligned hydroxyl groups directly interact with the specific plane of ice crystals.[9] The mutants A17L and A21L, where the substitution lies adjacent to the Thr-rich face, caused a significant decrement of thermal hysteresis activity.[10] NMR dynamics study of the wild-type and two inactive mutant AFPs, A17L and T13S/T24S, suggested that the α-helical structures of these three AFPs in solution are maintained at temperatures within the

**Table 1.** Exchange rate constants ($k_{ex}$, $s^{-1}$) and relative protection factors ($P_{rel}$) of the wt-, A17L-, and A20L-AFPs at 15 °C

| Imino | Wt-AFP | | A17L-AFP | | A20L-AFP | |
|---|---|---|---|---|---|---|
| | $k_{ex}$ | $P_{rel}$ | $k_{ex}$ | $P_{rel}$ | $k_{ex}$ | $P_{rel}$ |
| S4 amide | 9.2±1.7 | 1 | 15.1±3.3 | 0.6 | 11.1±1.0 | 0.8 |
| N16/N27 amide | 3.9±0.8 | 1 | 5.0±2.7<br>8.1±2.3 | 0.8<br>0.5 | 3.8±0.7<br>4.4±0.3 | 1.0<br>0.9 |
| N16/N27 Hδ21 | 0.6±0.6 | 1 | 1.6±0.6<br>1.0±1.1 | 0.4<br>0.6 | 0.9±0.7 | 0.7 |
| N16/N27 Hδ22 | 1.5±0.3<br>1.6±0.7 | 1 | 2.8±1.1<br>3.8±1.6 | 0.5<br>0.4 | 1.9±0.5 | 0.8 |
| R37 Hη | 51.4±3.3 | 1 | n.a.[a] | < 0.2 | 105.7±7.2 | 0.5 |

[a]Not available.

thermal hysteresis gap.[16]

Here, we first found that the inactive mutant A17L-AFP displays unique feature in hydrogen exchange, in contrast to wild-type AFP or the active mutant A20L-AFP. It was reported that the flexibility of the C-terminal region causes a loss of thermal hysteresis activity because its dynamic nature strongly prevents binding to the ice surface.[12] These results were strongly correlated with our finding that the R37-Hη protons, located at the C-terminals of wt- and A20L-AFPs, have much smaller $k_{ex}$ values than that of the A17L-AFP at 15 °C (Table 1). In addition, the amide proton of the S4 residue, which is close to the N-terminal in type I AFPs, also shows similar hydrogen exchange behavior (Fig. 3). Thus, our study conclusively demonstrates the previous suggestion that the helical stabilization of N- and C-termini is the critical component for antifreeze activity of the type I AFP.

Previous X-ray crystallographic studies demonstrated that the type I AFP exhibits anti-parallel dimeric conformation *via* the intermolecular hydrophobic interaction between Ala-rich faces with Thr γ-methyl groups.[8] Based on this structure, AFPs could form the oligomeric conformation *via* continuous α-helical structure in solution. The relatively higher molecular weights of AFPs in solution can explain severe line-broadening of the 1D spectra of wt- and A17L-AFPs (Fig. 2). However, the A20L-AFP has relatively lower molecular weight compared to other two AFPs because the A-to-L mutation at position 20 interferes with formation of higher-order oligomeric conformation. Thus, the 1D spectra of the A20L-AFP looks more sharpening than those of other two AFPs (Fig. 2). This result indicates that the alanine residue at position 20 in the AFP locates on the dimerization surface.

The A-to-L mutation at position 20 had no effects on the hydrogen exchange of the certain protons of type I AFP. However, in contrast to A20L-AFP, the A-to-L substitution at position 17 severely affected the $k_{ex}$ values of certain protons in AFP. These results indicate that the bulky group of Leu residue at position 17 in the A17L-AFP causes the conformational flexibility and then increases the hydrogen exchange rates of certain protons. However, the bulky group of Leu residue at position 20 did not affect the conformational flexibility. Because of the dynamic nature of the A17L-AFP, this AFP weakly bind to ice crystal compared to the wt- and A20L-AFPs. This weak binding of A17L-AFP cannot prevent growth of the ice crystal, so that the A17L-AFP has no thermal hysteresis effects in contrast of other two AFPs.

In summary, our study shows that wt-AFP and the active mutant A20L-AFP, exhibit relatively slow exchange of certain exchangeable protons compared to the inactive mutant A17L-AFP. Based on this hydrogen exchange study, we suggest that A17L-AFP, compared to wt- and A20L-AFPs, exhibit unique feature in hydrogen exchange with solvent water. The dynamic property of the type I AFP may be a key feature necessary to achieve wild-type thermal hysteresis activity.

**Acknowledgments.** This work was supported by the NRF grants [2010-0020480, 2012-R1A4A1-027750 (BRL)] funded by the Korean Government (MEST). This work was also supported by a grant from Next-Generation BioGreen 21 Program (SSAC, no. PJ009041), Rural Development Administration, Korea. We thank the GNU Central Instrument Facility for performing the NMR experiments.

## References

1. Davies, P. L.; Hew, C. L. *FASEB J.* **1990**, *4*, 2460.
2. Harding, M. M.; Ward, L. G.; Haymet, A. D. *Eur. J. Biochem.* **1999**, *264*, 653.
3. Liu, Y.; Li, Z.; Lin, Q.; Kosinski, J.; Seetharaman, J.; Bujnicki, J. M.; Sivaraman, J.; Hew, C. L. *PLoS One* **2007**, *2*, e548.
4. Miura, K.; Ohgiya, S.; Hoshino, T.; Nemoto, N.; Suetake, T.; Miura, A.; Spyracopoulos, L.; Kondo, H.; Tsuda, S. *J. Biol. Chem.* **2001**, *276*, 1304.
5. Gauthier, S. Y.; Scotter, A. J.; Lin, F. H.; Baardsnes, J.; Fletcher, G. L.; Davies, P. L. *Cryobiology* **2008**, *57*, 292.
6. Yeh, Y.; Feeney, R. E. *Chem. Rev.* **1996**, *96*, 601.
7. Patel, S. N.; Graether, S. P. *Biochem. Cell Biol.* **2010**, *88*, 223.
8. Sicheri, F.; Yang, D. S. *Nature* **1995**, *375*, 427.
9. Zhang, W.; Laursen, R. A. *J. Biol. Chem.* **1998**, *273*, 34806.
10. Baardsnes, J.; Kondejewski, L. H.; Hodges, R. S.; Chao, H.; Kay, C.; Davies, P. L. *FEBS Lett.* **1999**, *463*, 87.
11. Low, W. K.; Lin, Q.; Hew, C. L. *J. Biol. Chem.* **2003**, *278*, 10334.
12. Patel, S. N.; Graether, S. P. *Protein Sci.* **2010**, *19*, 2356.
13. Hong, J.; Hu, Y.; Li, C.; Jia, Z.; Xia, B.; Jin, C. *PLoS One* **2010**, *5*, e15682.
14. Bai, Y.; Sosnick, T. R.; Mayne, L.; Englander, S. W. *Science* **1995**, *269*, 192.
15. Graether, S. P.; Slupsky, C. M.; Sykes, B. D. *Proteins* **2006**, *63*, 603.
16. Graether, S. P.; Slupsky, C. M.; Davies, P. L.; Sykes, B. D. *Biophys J.* **2001**, *81*, 1677.